Economic Viability of Using Thermal Energy Storage for Flexible Carbon Capture on Natural Gas Power Plants

Braden J. Limb[1], Ethan Markey[1], Roberto Vercellino[1], Shane Garland[1], Maxwell Pisciotta[2], Peter Psarras[2], Daniel R. Herber[1], Todd Bandhauer[1], and Jason C. Quinn[†1]

[1]Colorado State University, Fort Collins, CO, 80523
[2]University of Pennsylvania, Philadelphia, PA, 19104
[†]Author Contact: Email: jason.quinn@colostate.edu
Address: Department of Mechanical Engineering, 1374 Campus Delivery, Colorado State University, Fort Collins, CO 80523, United States

Abstract

Fossil fuel-based power plants generate 80% of the electricity in the United States and provide a reliable generation source for both base and peak power demands. These plants are expected to adapt to changes in environmental policies that will require carbon management with carbon capture and storage (CCS) representing a possible solution. Current solvent-based CCS has a detrimental impact on a power plant's performance due to large heat loads required for carbon capture solvent regeneration. This parasitic load restricts the power plant's output and operation flexibility. Therefore, this study evaluates the feasibility of using thermal storage technologies for natural gas combined cycle (NGCC) power plants coupled with CCS to minimize the impact of solvent regeneration and enable the plant to operate at peak power output. Thermal storage can minimize the impact of CCS on the power plant by providing the heat load required for solvent regeneration during times of peak demand which will allow the plant to operate unrestricted and at full power. In total, fifteen unique thermal storage configurations were evaluated from three thermal storage categories: Brayton cycle heat pump, vapor compression heat pump, and heat recovery steam generator steam extraction for storage. The viability of these systems was determined by evaluating each configuration on thousands of real-world Locational Marginal Pricing (LMP) profiles from the New York Independent System Operator and California Independent System Operator electricity markets using a techno-economic analysis. Results were compared to the performance of a base power plant (NGCC with CCS and no thermal storage) to determine the impact of thermal storage on power plant economics. Overall, six of the thermal storage configurations performed better than base CCS enabled power plant on between 11.5% - 38.7% of the LMP signals evaluated. The best performing configuration was a vapor compression heat pump that used flue gas as the working fluid and had both hot and cold thermal storage units. This configuration performed better than the base CCS power plant on 38.7% of the LMP profiles. The results of this study show thermal storage can mitigate the economic impact of carbon capture solvent regeneration on NGCC power plants. Discussion focuses on the impact of electricity pricing on the optimal thermal storage system, the advantages and disadvantages of the systems evaluated, and identifies limitations with the study.

Keywords

Natural Gas Power Plant; Emissions Reduction; Thermal Energy Storage; Techno-economic analysis

Nomenclature

Acronyms:

ARPA-E	DOE's Advanced Research Projects Agency–Energy
ATB	NREL Annual Technology Baseline
CAISO	California Independent System Operator
Case B31B	NGCC + CCS power plant specified by NETL
CCS	Carbon Capture and Storage
CO_2	Carbon Dioxide
DOE	Department of Energy
EES	Engineering Equation Solver
EIA	U.S. Energy Information Administration
HRSG	Heat Recovery Steam Generator
IPT	Intermediate Pressure Turbine
LMP	Locational Marginal Pricing
LPT	Low Pressure Turbine
NETL	National Energy Technology Laboratory
NGCC	Natural Gas Combined Cycle
NGCC+CCS	NGCC Power Plant with Carbon Capture and Storage
NGCC+CCS+TES	NGCC Power Plant with Carbon Capture and Storage and Thermal Energy Storage
NPV	Net present value
NYISO	New York Independent System Operator
TES	Thermal Energy Storage

Thermal Storage Configuration Abbreviations:

Brayton	Brayton Cycle Heat Pump
FG	Flue gas as working fluid
FG_A	Flue gas heated air as working fluid
FG_S	Flue gas heated steam as working fluid
H	Hot thermal storage
HC	Hot and cold thermal storage
HRSG IPT	Steam extraction from the intermediate-pressure turbine in the heat recovery steam generator for storage
HRSG LPT	Steam extraction from the low-pressure turbine in the heat recovery steam generator for storage
S	Steam as working fluid
S_S	Steam heated steam as working fluid
Tiered VC	Tiered vapor compression heat pump with interconnected hot and cold storage

1. Introduction

Across the world there are a multitude of climate goals designed to reduce the impact of global warming in the coming years. Most of these goals center around reducing greenhouse gas emissions, particularly carbon dioxide (CO_2) [1–4]. Currently, fossil fuel based electricity generation is the largest greenhouse gas emitter of all the economic sectors at 25% of total global emissions [5]. To meet future environmental goals, fossil fuel-based power plants will require the addition of carbon capture and storage (CCS) to reduce their overall environmental impact [6–10]. However, the seamless integration of CCS systems has a variety of hurdles.

One major challenge with the integration of CCS is related to the operation of the power plant. At this time, the real-world feasibility of CCS has only been demonstrated a couple of times on base load power plants fueled by coal and natural gas [11,12]. In the last decade, 121 base load coal fired power plants have been decommissioned or converted to natural gas due to stricter emissions standards and economic constraints [13,14]. Additionally, nuclear plants are not being deployed because of safety concerns, policy changes, and high initial capital costs [15–17]. These plants are being replaced by less expensive renewable generation technologies (i.e. solar and wind) which have intermittent production issues and limited operation flexibility. As environmental policies continue to be adopted and the fraction of renewables increases, it is expected that natural gas power plants with CCS will serve as a technology to replace coal and nuclear loads while also meeting peak demands when renewable energy is not available [18,19]. However, the operation of CCS systems requires a large parasitic heat load from the power plant for the carbon capture solvent regeneration process [20]. This solvent regeneration process is essential to separate and store the captured CO_2 from the chemical-based solvent, but in doing so requires an immense amount of heat from the power plant. The heat load in this process is traditionally supplied via steam taken from the heat recovery steam generator (HRSG) in the natural gas combined cycle (NGCC) power plant. This reduces the power plant's power output to the grid since less steam can be used for power generation in the steam turbines. Overall, this load can reduce the total power generation by 12%, limits the plant's operating flexibility, and reduces the peak power output of the plant. In a scenario where renewable technologies are fully deployed, it is expected that natural gas plants will only represent 3% of the total power generation sector and will primarily be used for highly variable peaking demands caused by the intermittency of renewable technologies [21,22]. This flexible operational mode represents a major challenge to traditional CCS systems which have only been operated on baseload power systems.

Since future power plants will need to incorporate CCS technologies, there is a need to evaluate technologies that can work synergistically with power plants using CCS to overcome the operational limitations caused by carbon capture. Currently, two areas of research are focused on addressing these concerns: CCS bypass and fluid/energy storage. One of the most studied methods to increase CCS flexibility is to bypass the CCS unit during peak loads [23–28]. This allows the power plant to operate at full power output, but also releases all combustion gases to the environment. Studies have shown that bypassing the CCS is only economically feasible in situations where carbon taxes are between \$20-70/ton-CO_2 which is below expected targets [27,29–31]. As such, bypass is expected to have minimal deployment in future grids [25]. The

second area of research aimed at mitigating CCS operation constraints is the use of storage technologies. The primary storage technologies that have been evaluated include solvent storage, hydrogen storage, and oxygen storage [23–28,32–36]. The main benefit of solvent storage is that it allows the energy intensive process of solvent regeneration to be shifted to off-peak power periods. The solvent storage tanks are charged or discharged depending on the operation of the power plant and the energy available for solvent regeneration. During times of peak power demand, the CCS solvent absorbs CO_2 from the flue gas and then stores the solvent in a storage tank. During times of low power demand, the storage tank discharges the CO_2 rich solvent for solvent regeneration using excess plant power. Studies have shown solvent storage to increase plant profits by 9-29% compared to systems without solvent storage [27]. However, solvent storage solutions require specialty equipment which increases capital costs and makes them infeasible in future market conditions [25,37]. Two additional methods to increase flexibility of CCS include hydrogen and oxygen storage [32–36]. Both hydrogen and oxygen storage shows promise by taking advantage of electricity price arbitrage. Hydrogen and oxygen can be produced and stored using low-cost electricity, then burned to produce additional electricity and profits at high prices. These storage methods show economic promise, but have limited real world testing which has led to concerns about their feasibility [38]. Another storage technology that has shown significant economic promise is thermal energy storage (TES). Previous studies have found TES to have promising economic potential to stabilize the electricity grid, increase NGCC peak power generation, and increase NGCC combustion efficiency through inlet chilling [39–51]. However, the interconnection between TES and CCS has not been explored. Therefore, this study evaluates the feasibility of TES solutions to be used in combination with NGCC power plants and CCS technologies.

TES systems can be made up of both hot and cold thermal storage units and provide many benefits to the NGCC+CCS system. First, hot thermal storage can be used to supply steam to the CCS regeneration process during times of peak power demand which eliminates the steam requirement from the NGCC and therefore increase the NGCC's power output to the grid. Second, cold thermal storage can be generated concurrently with hot thermal storage using a Brayton Cycle heat pump or tiered vapor compression heat pump. This cold energy can be used to chill the air entering the NGCC power plant which increases the inlet air's density, thus improving the plant's efficiency and net power output [39]. Third, future electricity grids are expected to have large price variability which TES systems can leverage [52,53]. TES units can charge during times of low electricity demand (low electricity prices) and discharge during peak demand (high electricity prices) which increase overall power plant profits since more power will be output at higher electricity costs. Lastly, the charging and discharging of the TES system allows the power plant to have a more flexible power output range (i.e. lower minimum power output and higher maximum power output) than comparable NGCC+CCS systems. This research evaluates multiple TES configurations (Brayton cycle heat pump, vapor compression heat pump, and HRSG steam extraction for storage) over thousands of real-world electricity price signals to determine the optimal thermal storage solution to overcome current limitations with NGCC+CCS systems. Discussion focuses on the impact of electricity pricing on the optimal thermal storage system, the advantages and disadvantages of the systems evaluated, and identifies limitations with the study.

2. Methods

The methods are broken down into the four subsections representing the components necessary for the completion of this analysis. The first subsection details the fifteen unique thermal storage configurations that were evaluated for this study. Evaluation of the proposed thermal storage technologies required three interconnected models to simulate the power plant's operation and evaluate the economic feasibility of TES coupled with NGCC+CCS. These models include a technology model which simulates the thermodynamic performance of each of the key components (NGCC, CCS, and TES), an economics model which evaluates the NPV of the system based off the profits and costs (including all capital and operational costs), and an operation model which determines how the power plant should operate based off a given electricity price signal. Descriptions of the each of these models are presented in subsections two through four.

2.1. Thermal Energy Storage Configurations

In total, fifteen unique thermal storage configurations coupled with a NGCC+CCS were evaluated for this study. These configurations were identified through a preliminary economic and thermodynamic analysis that confirmed real-world feasibly. The configurations are broken down into 3 main categories of thermal storage heat pump design: Brayton cycle heat pump, vapor compression heat pump, and HRSG steam extraction for storage (Figure 1). Regardless of the thermal storage category used, all configurations interact with the NGCC+CCS in a similar way. Each configuration stores thermal energy during times of low electricity prices and discharges that thermal energy during high electricity prices to generate maximum profits. In all cases, hot thermal energy is taken from the NGCC plant or generated using electricity to charge the hot TES. The hot TES is discharged to provide steam to the CCS unit for solvent regeneration such that the NGCC can output maximum power to the grid. If used, cold TES is charged using electricity and discharged to chill NGCC inlet air which increases combustion efficiency. The main operational difference between the unique configurations is the thermal energy source or generation method. The thermal energy source or generation method is based on the combination of thermal storage category, working fluid, and hot and/or cold thermal storage that is used. A list of all the thermal storage configurations is presented in Table 1.

Each TES configuration shown in Table 1 has been designated a simplified name for reference in this paper. Each name starts with the heat pump type, followed by the working fluid used, and finishes with a designation for the type of thermal storage used (hot and/or cold). The heat pump types used are Brayton cycle heat pump (Brayton), vapor compression heat pump (Vapor), tiered vapor compression heat pump with interconnected hot and cold storage (Tiered VC), steam extraction from the low-pressure turbine in the heat recovery steam generator for storage (HRSG LPT), and steam extraction from the intermediate-pressure turbine in the heat recovery steam generator for storage (HRSG IPT). The working fluids used are flue gas (FG), steam (S), flue gas heated air (FG_A), flue gas heated steam (FG_S), and steam heated steam (S_S). Lastly, there were two types of thermal storage used: hot storage (H) or hot and cold storage (HC). For example, Brayton – A/HC is a Brayton cycle heat pump that uses ambient air as the working fluid and has both hot and cold storage. This cycle differs from Brayton – FG_A/HC in that Brayton – FG_A/HC is a Brayton cycle heat pump that also uses air as the working fluid, but it is preheated by the flue gas leaving the HRSG before entering the Brayton cycle. For all vapor

compression (besides Tiered VC – S/HC) and HRSG configurations that use both hot and cold storage, a vapor compression unit is used to generate the cold thermal energy for inlet chilling.

Table 1. Breakdown of each of the thermal storage configurations evaluated in this study. All systems are coupled with a natural gas combined cycle power plant with carbon capture sequestration for evaluation.

Name	***Heat Pump Type***	***Working Fluid***	***Hot***	***Cold***
Brayton - FG/HC	Brayton Cycle	Flue Gas	✓	✓
Brayton - FG/H	Brayton Cycle	Flue Gas	✓	×
Brayton - A/HC	Brayton Cycle	Ambient Air	✓	✓
Brayton - A/H	Brayton Cycle	Ambient Air	✓	×
Brayton - FG_A/HC	Brayton Cycle	Flue Gas Heated Air	✓	✓
Brayton - FG_A/H	Brayton Cycle	Flue Gas Heated Air	✓	×
Vapor - FG_S/HC	Vapor Compression	Flue Gas Heated Steam	✓	✓
Vapor - FG_S/H	Vapor Compression	Flue Gas Heated Steam	✓	×
Vapor - S_S/HC	Vapor Compression	Steam Heated Steam	✓	✓
Vapor - S_S/H	Vapor Compression	Steam Heated Steam	✓	×
Tiered VC - S/HC	Tiered Vapor Compression	Steam	✓	✓
HRSG LPT - S/HC	Steam from Low Pressure Turbine	Steam	✓	✓
HRSG LPT - S/H	Steam from Low Pressure Turbine	Steam	✓	×
HRSG IPT - S/HC	Steam from Intermediate Pressure Turbine	Steam	✓	✓
HRSG IPT - S/H	Steam from Intermediate Pressure Turbine	Steam	✓	×

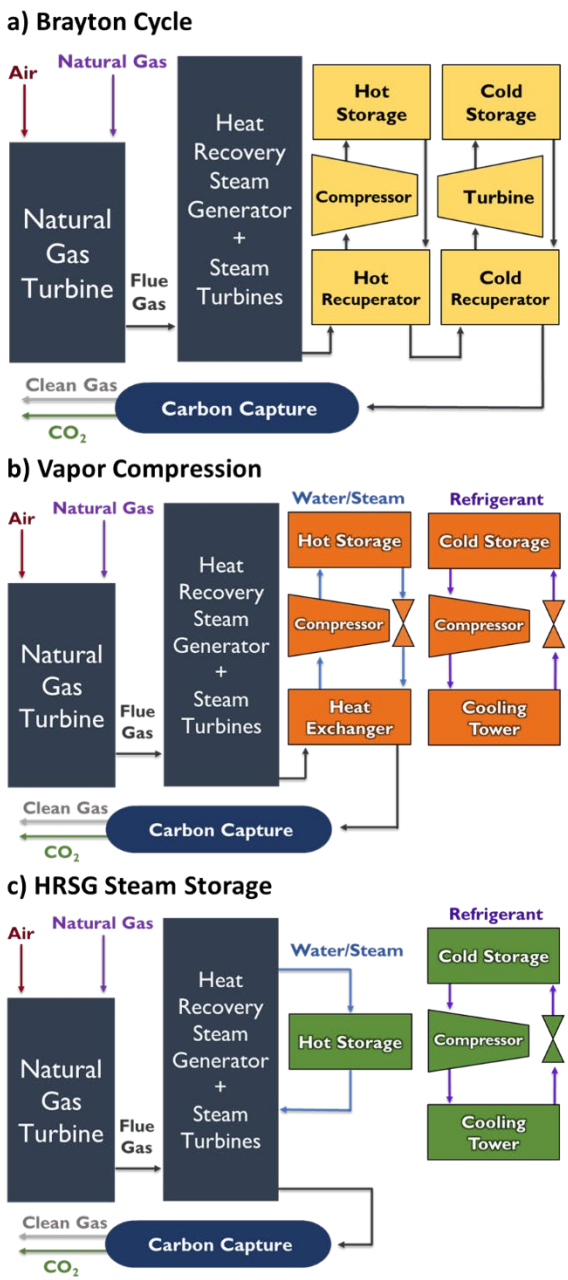

Figure 1. Three different thermal energy storage systems were considered (a) Brayton cycle heat pump, (b) vapor compression heat pump, and (c) steam storage from the heat recovery steam generator (HRSG).

Evaluation of the proposed thermal storage technologies required three interconnected models to simulate the power plant's operation and evaluate the economic feasibility of TES coupled with NGCC+CCS. These models include a technology model which simulates the thermodynamic performance of each of the key components (NGCC, CCS, and TES), an operation model which determines how the power plant should operate based off a given electricity price signal, and an economics model which evaluates the net present value (NPV) of the system based off the profits

and costs (including all capital and operational costs). Descriptions of the each of these models are presented in the following sections.

For this study, the NGCC+CCS+TES's operation phases were reduced to a "charge phase", a "discharge phase", a "neutral phase" and a "boost phase" (Figure 2). As defined, the "charge phase" references the time that power output is decreased, and the extra energy is used to charge the thermal storage reservoirs. The "discharge phase" refers to the operation mode where the peak power output is being sent to the grid and both thermal storage reservoirs are being depleted. The "neutral phase" refers to the operation mode where the power plant is running as a standard NGCC+CCS plant and no charging or discharging of thermal storage is taking place. Last, the "boost phase," which is only available for configurations that include cold storage, refers to the operation mode where the cold TES is simultaneously being charged and discharged. For some configurations, this results in a slight power boost above the neutral power output and incurs an increase in natural gas consumption.

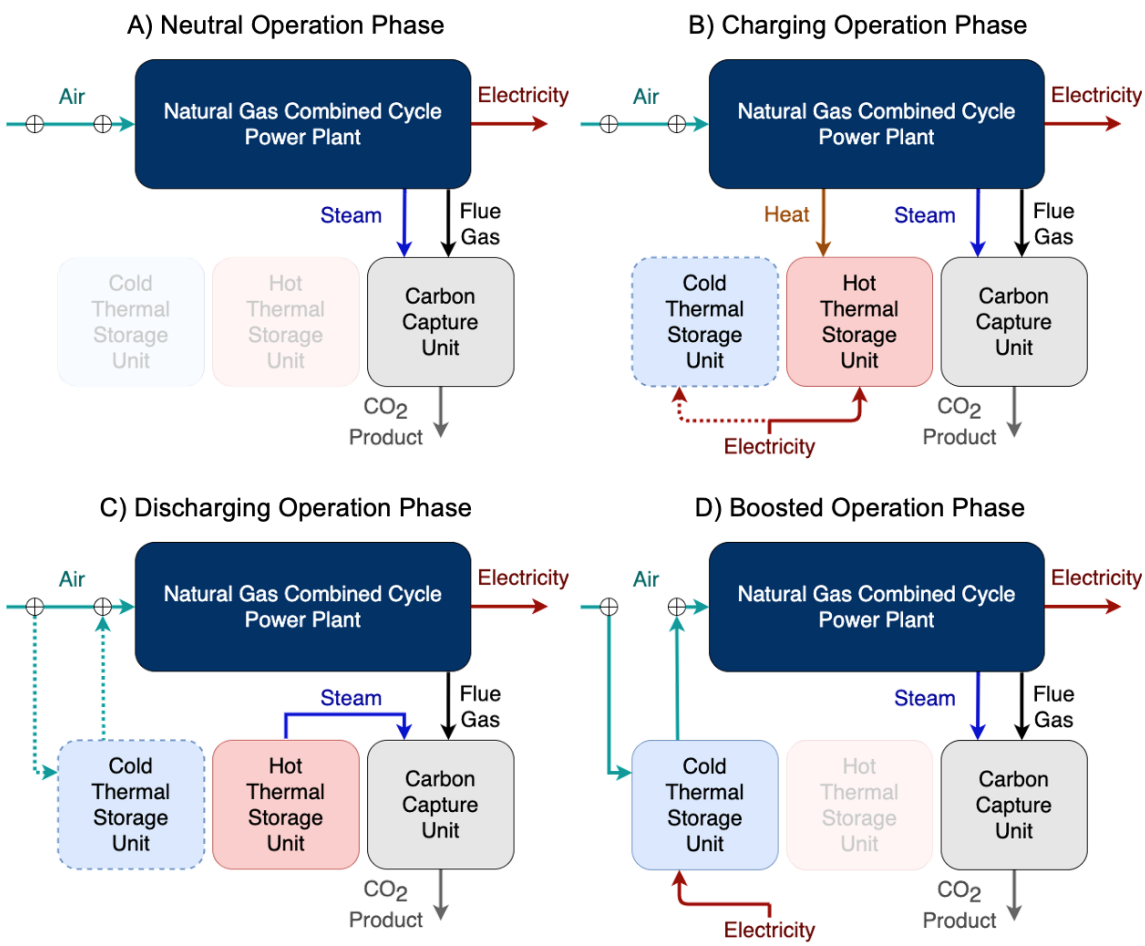

Figure 2. Four operation phases that were simulated for the thermal energy storage configurations evaluated: A) neutral operation phase, B) charging operation phase, C) discharging operation phase, and D) boosted operation phase (only available if cold TES is used). Dotted lines to/from cold thermal storage unit represent optional paths if cold TES is used. Cold TES is not required on all configurations.

2.2. Technology Model

The technology model is designed to simulate the key components of the NGCC+CCS+TES configurations in the different phases of operation. The following sections detail how each of the main components (NGCC, CCS, and TES) are modeled and validated.

2.2.1. Natural Gas Combined Cycle Power Plant + Carbon Capture Sequestration Modeling

The base power plant selected for this analysis was the NGCC power plant with CCS as specified in the National Energy Technology Laboratory's (NETL) 2019 report (Case B31B) [54]. Case B31B uses Shell's proprietary and patented CANSOLV CO_2 capture technology which utilizes a regenerable amine solvent [55]. As such, all assumptions listed for both the NGCC and CCS units in the NETL report were used for this analysis. The TES configurations were coupled with the base power plant and compared to the base power plant without TES to determine the value of TES used with CCS. A thermodynamic model of this plant was constructed in Engineering Equation Solver (EES) to properly represent the effect that each TES configuration has on the base plant's operation. This model calculates the heat transfer, power production/consumption, and thermodynamic states on either side of the primary components (heat exchangers, pumps, compressors, turbines, etc.) for both the gas and the steam cycles. The model assumes constant volumetric air flowrate, combustor temperature, heat of combustion, and component isentropic efficiencies. The net power output and flowrates of the gas and steam plant calculated in the model were compared to those specified by the NETL report. All calculated values were within 5% of the specified NETL value. The technology model governing equations, detailed process flow diagram, assumption list, and mass, power, and heat flows are included in the Supplementary Data for this paper. The CANSOLV CCS steam reboiler duty and electrical parasitic load (as specified by NETL) were held constant for all operation modes. Since the steam reboiler duty is held constant, the percent of CO_2 sequestered was assumed to vary with natural gas flowrate according to data in the literature [56,57].

2.2.2. Thermal Energy Storage Modeling

In order to evaluate the TES configurations, models were created for each of the individual configurations. Like the base model, the surrogate models calculate the heat transfer, power consumption/production, and thermodynamic states of the main heat pump components, including the storage mediums, heat exchangers, compressors, turbines, expansion valves, and pumps. The surrogate models output the heat rate to/from the thermal storages, flow rates of the working fluids, total mechanical power required to run individual configurations, and sizes of each component. The process flow diagram, assumption list, and mass, power, and heat flows are included for configuration Vapor – FG_S/HC in the Supplementary Data as a representative case for all configurations.

The base NGCC+CCS model was modified to incorporate the charging and discharging modes of TES operation. During the charging mode, the working fluid streams in the base model were adjusted to account for the fluid extraction in the TES configuration and re-combination at the corresponding location in the base plant. For example, in the HRSG IPT – S/HC configuration steam is extracted from the intermediate-pressure turbine (IPT) inlet, condensed in the hot storage, pumped to a high pressure, and then recombined with the inlet to the HRSG. This results in lower flow rates through multiple components in the steam cycle, lower power outputs from

the IPT and low-pressure turbine (LPT), and higher HRSG steam inlet/gas outlet temperatures. The process flow diagram, assumption list, and mass, power, and heat flows are included in the Supplementary Data for HRSG IPT – S/HC to show the alterations to the base B31B model. During the discharging mode, the hot storage is used to provide the CANSOLV reboiler steam requirement. As such, the steam used for the CANSOLV reboiler during normal operation is instead routed through the LPT, consequently increasing power output for all configurations. The cold storage heat rate is used to calculate increased gas and steam flowrates. The total increase in gas and steam generator sizes and costs are calculated in discharging mode of the model.

The thermal storage medium assumed for this research was modular concrete blocks based on Storworks' BolderBloc™ Module [58]. Modular concrete blocks were selected due to their low cost and ability to be configurable with every thermal generation design. The thermophysical properties of pure concrete were assumed for modeling purposes (thermal conductivity of 0.5 W m^{-1} °K^{-1} and specific heat of 0.96 kJ kg^{-1} °K^{-1}) [59,60]. Additionally, it was assumed that the heat exchanger effectiveness was 0.85 and the required CCS reboiler steam temperature was 152°C. The focus of this study was to determine if adding TES to NGCC+CCS power plants was feasible, not to determine the best TES medium to use. Therefore, it is recommended that future work evaluate additional thermal storage mediums to determine if they can further optimize the NGCC+CCS+TES design and improve NPV.

2.3. Economic Model and Assumptions

A 30-year discounted cash flow analysis was used to evaluate which TES technology had the highest NPV based on simulations of the power plant using real-world electrical grid pricing. Standard economic assumptions are used and presented in Table 2 [61,62]. All dollar values were adjusted to December 2018 dollars based on historical inflation rates as calculated by the Bureau of Labor Statistics using the Consumer Price Index [63]. A full list of equations used to calculate the 30-year discounted cash flow analysis and the NPV can be found in the Supplementary Data.

Table 2. Economic Analysis Assumptions

Item	***Value***	***Units***	***Source***
Loan Interest Rate	5%		ATB
Loan Term	30	years	ATB
Financed Amount	80%		ATB
Equity Amount	20%		ATB
Construction Interest Rate	3.5%		ATB
Construction Period	3%	years	ATB
Construction Build Rate	80%, 10%, 10%		ATB
MACRS Depreciation	15%	years	ATB
Tax Rate (Federal and State)	25.7%		ATB
Internal Rate of Return	10%		ATB
Annual Natural Gas Price Increase	3.50%	%/year	EIA
Annual Electricity Price Increase	3.50%	%/year	EIA

Cost assumptions for each of the technologies varied by the individual components. Depending on the components that were added or removed for a given system, the prices of the components

were scaled accordingly. All costs associated with new TES components were based on the same components used within NETL's B31B power plant. Similarly, when the CCS unit was scaled to accommodate the higher power outputs, costs were scaled based off the CANSOLV system used for B31B. Lastly, thermal storage component costs were based on Storworks' project capital costs of $25/kW-thermal for a 100° K temperature change during charging/discharging [58]. Both fixed and variable operation costs were based on the values provided by NETL for Case B31B and scaled depending on the thermal storage configuration. All system components were assumed to last a 30-year life, except those replaced through routine maintenance.

To simulate real world performance of the NGCC+CCS+TES systems, electricity Locational Marginal Pricing (LMP) profiles were used. Real-world LMP data is available for the major wholesale electricity markets in the United States. For this analysis, the New York Independent System Operator (NYISO) and the California Independent System Operator (CAISO) electricity regions were used as the primary source for LMP profiles [64,65]. Natural gas fuel prices for the first year were assumed to be those reported in the New York and California regions over the 2018 calendar year as provided by U.S. Energy Information Administration [66].

Since the selected electricity LMP profiles and natural gas prices only represented one years' worth of data, the operation model outputs (revenue generated, operation costs, total profits, etc.) were duplicated for every subsequent year for the 30-year life of the system. To approximate increasing energy prices over time, the price increases of 3.5% annually and 2.2% annually were used for natural gas and electricity, respectively, as expected by the Energy Information Administration's Annual Energy Outlook 2020 [62]. Fixed and variable operation costs associated with the NGCC, CCS, and TES were assumed to remain constant over the 30-year life of the system.

2.4. Operation Model

The operation model simulates the behavior of the NGCC+CCS power plant by using the selected LMP profiles to make hourly dispatch decisions one day at a time. All simulations were performed using both the base power plant and the thermal storage configurations evaluated in this study. To simulate real world performance, the Operation Model coordinates whether to run the NGCC system and when it is most profitable to operate the different phases of the TES with a series of decisions (Figure 3). To do this, the model first calculates the breakeven electricity price. The breakeven electricity price correlates to the minimum price where the plant becomes profitable given specified fuel and operation costs. Next, the daily prices higher than the breakeven price are selected and sorted in an ascending manner. Charging of the TES is assigned to the lowest prices and discharging is assigned to the highest prices. This decision is then validated by comparing the profit made by charging and discharging the TES verses the profits of running the plant in the neutral phase. If charging/discharging the TES does not generate additional revenue, the operation mode is reverted to neutral operation. Finally, for the hours when the plant is neither charging or discharging the model evaluates whether the boost phase could be more profitable and adjusts the operations accordingly. The operation model also evaluates whether running the plant during those hours is profitable at all, finalizing the operation scheme for the day and moving on to the next day.

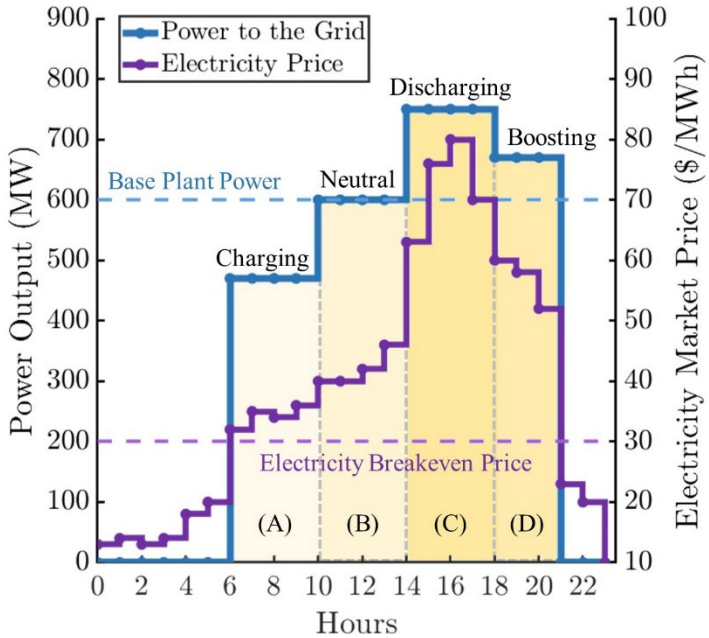

Figure 3. Operation phases of the power plant as determined by the operation model. Section (A) shows the "Charging" operation mode which occurs at low electricity prices and decreased power output with the remaining power being used to charge the thermal storage units. Section (B) shows the power plant in "Neutral" operation with normal power output when electricity prices are neither high nor low. "Neutral" operation is the same as a plant operating without thermal storage. Section (C) shows the power plant in "Discharging" operation which occurs at high electricity prices and has increased power output due to the thermal storage units being discharged. Section (D) represents the "Boosting" operation mode which occurs when electricity prices are high, but it's not economical to run in "Discharging" mode. During the Boost phase of operation, the cold TES is being charged and discharged simultaneously which has a net increase in power output and natural gas fuel consumption.

3. Results and discussion

The results are broken down into the five subsections representing each step of the analysis. The first subsection details the cost breakdown of each of the thermal storage configurations. The second subsection details which configurations performed the best when compared to NETL's B31B over the NYISO electricity LMP profiles. The third subsection provides a cost sensitivity analysis to each of the main components used in the thermal storage configurations. The fourth subsection details the impact of electricity LMP profiles on the different configurations with discussion focused on the potential impact of future electricity markets. The fifth section provides a discussion on the limitations associated with this study.

3.1. Capital Cost Results

This section details a capital cost breakdown for each of the fifteen thermal storage configurations. As mentioned in section 2.2, the base power plant used in this study was the NGCC+CCS power plant (Case B31B) from the 2019 NETL report [54]. The total capital cost of each configuration includes the cost of the base power plant, the cost of the components used for TES (the storage medium, compressors, turbines, heat exchangers, etc.), and the cost differential between the current B31B generators and those required for the increased power output due to TES cold discharge. The costs associated with the base NGCC power plant and its CANSOLV

CCS system are $537 million and $745 million, respectively. Therefore, the total cost of B31B was $1.28 billion before the additional thermal storage components and larger generator sets (if needed) were added. Figure 4 details the capital cost breakdown of each of the TES configurations excluding the base power plant. Power plant costs were excluded because those costs do not change between the different TES configurations. The breakdown shown in Figure 4 includes all TES components (the storage medium, compressors, turbines, heat exchangers, etc.), and the cost differential between the current B31B generators and those required for the increased power output due to TES cold discharge. The following paragraphs detail the cost and component differences between each of the thermal storage categories that contribute to the overall cost of the systems.

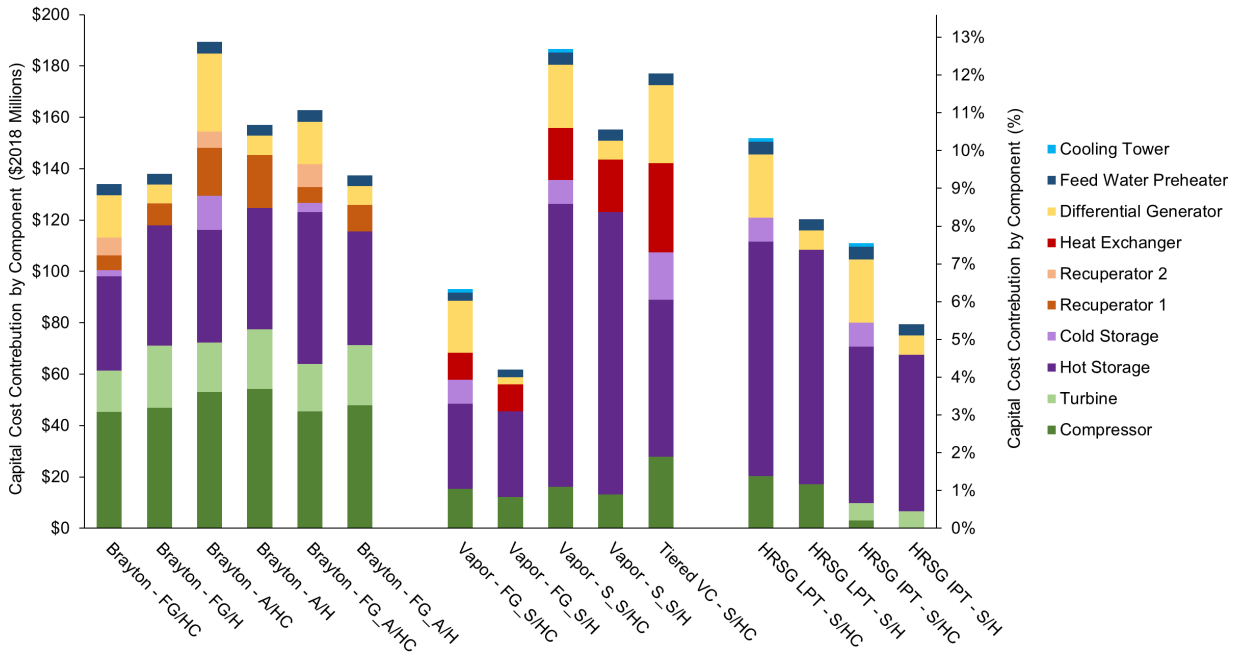

Figure 4. Capital cost breakdown by component for each thermal storage configuration. The thermal systems are integrated with a NGCC+CCS system which has a total capital cost of $1.28 billion. Secondary axis shows the percent of the total capital costs (including NGCC+CCS) that each thermal energy storage configurations make up.

The largest capital cost contributors for the Brayton cycle configurations are the compressor, the turbine, and the hot thermal storage. Brayton cycle configurations have a much larger compressor and turbine than vapor compression and steam extraction TES options because of the larger flow rates in these systems. Contrary to the vapor compression and steam extraction TES options which all use steam as the working fluid, the Brayton cycle configurations use flue gas or air as the working fluid. Since the working fluid is a gas, all the heat transfer is sensible and requires much higher flow rates and pressure ratios. These high flow rates and pressure ratios result in larger and more expensive turbines and compressors to be used. Overall, the Brayton cycle configurations varied in price from $134 million for flue gas option with both hot and cold storage to $189 million for the ambient air option using both hot and cold storage. While the latter configuration is the most expensive, it also has the flexibility of operating independently of the power plant and can take advantage of very low electricity prices for TES charging.

The largest capital cost contributor for the vapor compression heat pump configurations is the hot thermal storage. The vapor compression configurations suffer high storage costs because the steam used to heat the hot storage is close in temperature to the minimum steam temperature required by the CANSOLV reboiler. This small temperature difference requires a large thermal storage mass to extract the necessary energy from the inlet steam. Consequently, the larger the thermal storge mass, the larger the capital costs of the TES unit. The vapor compression heat pump configurations varied significantly in price from $61 million for the low-cost flue gas version to $186 million for the high-cost steam model. This large price difference stems from two principles. The first is that TES in the configuration utilizing flue gas allowed a larger temperature difference than that using steam, which results in smaller storage costs, as described above. The second principle is that the configuration utilizing flue gas is constrained by the amount of heat that it can extract from the flue gas, which means that the total amount of energy stored in the hot storage is less, and all component sizes are smaller than the configuration using steam.

The largest cost contributor for the HRSG steam extraction configurations is the hot storage. Similar to the vapor compression configurations, the steam extraction configurations suffer high storage costs because the steam used to heat the hot storage is close in temperature to the minimum storage temperature required by the CANSOLV reboiler. This small temperature difference requires a large storage mass to extract the necessary energy. The HRSG steam configurations have capital costs ranging from $80 million for the intermediate pressure turbine model with only hot storage to $152 million for the for the low-pressure turbine version with hot and cold storage. The differences between the cheapest and most expensive steam extraction configurations are the addition of cold storage, increase in generator size, and the increased compressor and hot thermal storage costs since the LPT steam is a lower quality (lower temperature and pressure) than the IPT steam.

As will be shown in the next section, the final NPV of each of these configurations is significantly impacted by the capital costs. This is because capital costs have a higher weighting factor in the discounted cash flow analysis than annual operation costs and revenue because capital costs are spent in the first few years of operation. Notably, all the thermal storage components make up less than 13% of the total NGCC+CCS+TES capital costs for every configuration evaluated.

3.2. Thermal Storage Downselection

The goal of this study was to determine the economic viability of adding TES to an NGCC+CCS system. In order to understand the economic viability of the TES configurations, the NPV of each NGCC+CCS+TES configuration was compared to the base NGCC+CCS power plant over real-world LMP profiles. The comparison between NPVs of the base plant and TES configurations is shown in Figure 5. This figure presets a range of NPVs for each TES configuration evaluated on NYISO nodes using box and whisker plots. The bounds of the box in the box and whisker plot represents the 25th and 75th percentile results. The base NGCC+CCS power plant was found to have a range of NPVs from -$1.15 billion to $41.9 million. All thermal storage configurations were evaluated with Figure 5 showing the net improvement compared to

the base plant. Scenarios that have a higher NPV than the base plant fall above the breakeven line and data points that fall below the breakeven line have a lower NPV. In order to be economically viable, the TES configurations need a portion of the results to fall above the breakeven line.

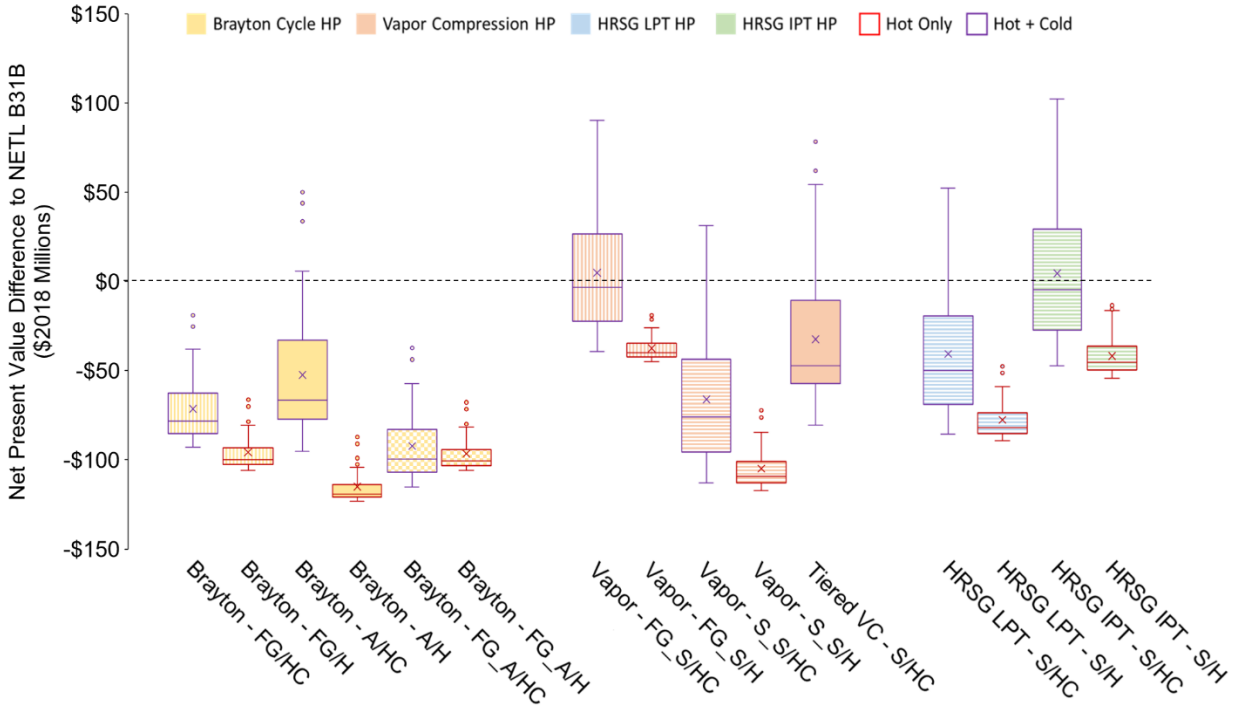

Figure 5. Net Present Value difference between each thermal storage configuration and NETL's B31B based on simulation with NYISO nodal data.

In general, the Brayton cycle configurations yielded lower NPVs than the base power plant due to their large capital costs. Of the Brayton cycle options, the configuration using air as the working fluid with both hot and cold storage (Brayton – A/HC) performed the best. It had a higher NPV than the base plant on 12.6% of the NYISO LMP profiles, the fifth highest percentage of the configurations evaluated. This configuration performed better than the other Brayton cycle configurations because it was able to charge the thermal storage independently of the power plant's operation. In order to charge the other configurations, the power plant needed to be in operation as they used heat from the NGCC flue gas or steam to heat the TES working fluid. Conversely, Brayton – A/HC pulls electricity directly from the grid and uses ambient air as the working fluid. Therefore, it is capable of charging at electricity prices lower than the breakeven cost of NGCC operation and the other Brayton cycle configurations. Charging independently of the NGCC power plant is particularly helpful in locations of low electricity prices and low NGCC capacity factors. That being said, the large capital costs of all the Brayton cycle configurations limited the overall benefit that was seen from the TES system. While this configuration was not the best performing overall due to high capital costs, it indicated that having a TES option capable of charging independent of the base plant could be valuable.

Based on the Brayton cycle results, a tiered vapor compression heat pump (Tiered VC – S/HC) was designed. This configuration uses interconnected vapor compression cycles to achieve the hot and cold temperatures required of the CCS and NGCC, respectively. Tiered VC – S/HC had a higher NPV than the base plant on 15.7% of the NYISO LMP profiles evaluated, the third highest percentage of the TES configurations. Tiered VC – S/HC performed better than Brayton – A/HC primarily due its lower capital costs. Both Vapor Compression heat pumps that included hot and cold thermal storage (Vapor – FG_S/HC and Vapor – S_S/HC) performed better than the base power plant over some of the NYISO profiles. The vapor compression configuration using steam as the working fluid and both hot and cold storage (Vapor – S_S/HC) performed similarly to the best Brayton cycle configuration with 11.5% of the nodes having a higher NPV than the base plant, the sixth highest percent of the configurations evaluated. The other vapor compression configuration (Vapor - FG_S/HC) had the highest NPVs of all the configurations evaluated. This configuration had a higher NPV than the base plant on 38.7% of the NYISO profiles. This can be attributed to the configuration's low capital cost and ability to utilize waste heat from the plant.

The thermal storage configuration using steam extraction from the intermediate pressure turbine in the HRSG with both hot and cold storage (HRSG IPT – S/HC) was the second-best performing configuration. It had a higher NPV than the base plant on 36.9% of the LMP profiles. Additional benefits to this configuration include: the simple design, low capital cost, and that it does not require additional power to run compressors during TES charging. The low-pressure turbine HRSG configuration with both hot and cold storage (HRSG LPT – S/HC) performed the fourth best in this analysis by having a higher NPV than the base plant on 13.7% of the nodes.

In addition to the evaluation over NYISO LMP profiles, the same analysis was performed on CAISO LMP profiles. However, the best performing configurations did not change during this analysis. Vapor – FG_S/HC and HRSG IPT – S/HC were the best performing configurations on the CAISO nodes. These two configurations had a higher NPV than the base plant on 28.3% and 27.8% of CAISO LMP profiles, respectively. Tiered VC – S/HC once again had the third highest percent of LMP profiles with a higher NPV than the base plant at 24.6%. Brayton – A/HC performed fourth best of the configurations by having a higher NPV than the base plant on 20.7% of the CAISO nodes. The main takeaway from the CAISO analysis is that the two TES configurations that can charge independently of the NGCC (Tiered VC – S/HC and Brayton – A/HC) increased their performance compared to the NYISO results, whereas the configurations dependent on NGCC performed worse in CAISO than in NYISO. This is because CAISO LMP profiles have a lower average electricity cost than the NYISO LMP profiles which decreases the overall capacity factor of the NGCC and limits the charging/discharging window of the TES configurations dependent on the NGCC's flue gas or steam for heat. Full results for the CAISO LMP analysis can be found in the Supplementary Data.

These results show that the thermal storage configurations with the lowest capital costs tend to perform the best across the price signals evaluated. Even though HRSG IPT – S/HC has higher capital costs than Vapor – FG_S/HC, it has a higher max power output and boost phase power which allows it to nearly make up for the difference in capital costs with the additional revenue

that it generates. Based on these results, Vapor – FG_S/HC, HRSG IPT – S/HC, and Tiered VC – S/HC are the best potential technologies to overcome the operational limitations caused by the large heat load needed for CCS solvent regeneration on NGCC power plants. Vapor – FG_S/HC and HRSG IPT – S/HC will be kept in future analysis because they performed the best overall and Tiered VC – S/HC will be kept because it adds the flexibility of charging independently of the power plant which could be important for future electricity LMP profiles where NGCC power plants are expected to operate with a lower capacity factor [67–69]. As mentioned previously, having a lower capacity factor will limit the time window where charging and discharging of the TES can take place for configurations dependent on heat from the NGCC. Configurations independent of the NGCC can operate more easily because they only need to discharge the TES when the NGCC is in operation.

3.3. Capital Cost Sensitivity

In order to ensure that the capital cost assumptions made for the different thermal storage configurations did not alter the results, a sensitivity analysis was performed. This sensitivity analysis was designed to show the impact of varying the capital cost of each thermal storage component by ±10% from its assumed cost, Figure 6. Only the impact of storage costs, differential generator costs, turbine costs, compressor costs, and recuperator costs are shown in Figure 6, because the other thermal storage components had a negligible impact on the overall NPV of the system. Additionally, these results are only shown for the Kensico Reservoir NYISO node which was found to be the median performing node for the configurations evaluated.

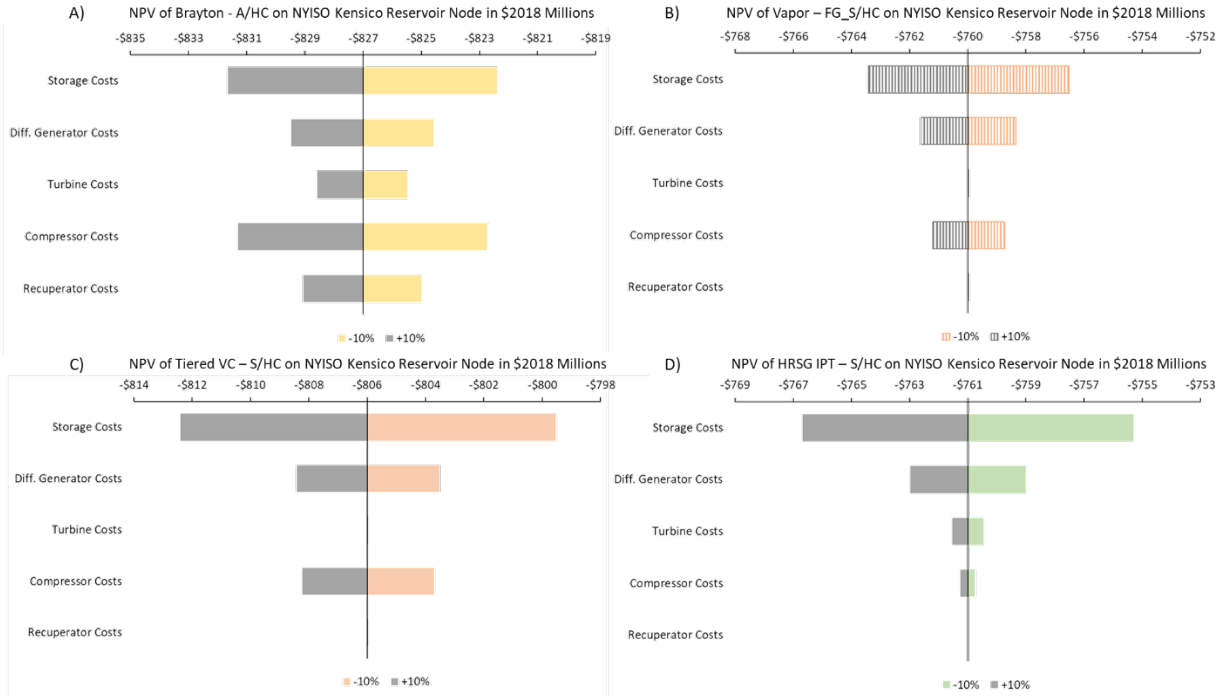

Figure 6. Capital cost sensitivity results for the 4 best performing thermal storage configurations determined. These configurations are A) Brayton - A/HC, B) Vapor – FG_S/HC, C) Tiered VC – S/HC, and D) HRSG IPT - S/HC. Results show the impact on NPV by adjusting the capital components of those specified by +/- 10%. The impact of changing capital costs of other components was found to be negligible. The NPV sensitivity presented was by evaluating the NYISO LMP profile for Kensico Reservoir, NY which is the median node in terms of performance of all configurations evaluated.

In general, changing the TES' component capital costs by ±10% was found to have a minimal impact on NPV with all changes being less than 1%. However, the most sensitive component was found to be the thermal storage costs for all configurations evaluated. Results from the 4 best performing configurations in section 3.2 show that changing the thermal storage costs by ±10% adjusted the NPV by $3.4 million (0.45%) for Vapor – FG_S/HC, $5.7 million (0.75%) for HRSG IPT – S/HC, $6.4 million (0.80%) for Tiered VC – S/HC, and $4.6 million (0.56%) for Brayton – A/HC. Due to the small percentage change seen in NPV by this analysis, only configurations that have very similar NPV results could perform better or worse comparatively. For example, the results in Figure 6 show that Vapor – FG_S/HC and HRSG IPT – S/HC have a similar NPV for the NYISO Kensico Reservoir LMP profile at -$760 million and -$761 million, respectively. If the storage costs were decreased by 10%, this would reduce the NPV to -$756 million for Vapor – FG_S/HC and -$755 million for HRSG IPT – S/HC. Therefore, HRSG IPT – S/HC would go from performing worse than Vapor – FG_S/HC, to performing better than it. However, this phenomenon only occurs in scenarios when configurations have similar NPVs to start (<1%). Even if the capital cost of the different configurations were changed ±10%, the ranking of configurations would not change. Vapor – FG_S/HC and HRSG IPT – S/HC would be the two best performing configurations and Tiered VC – S/HC would remain the third best performing configuration. Tiered VC – S/HC will not perform better than Vapor – FG_S/HC or HRSG IPT – S/HC by solely changing the component capital costs because the difference in NPV between these configurations ($47 million) is an order of magnitude higher than change seen in this sensitivity analysis ($3 million).

These results show that the best performing configurations will not change if the capital cost approximations used in this study were off by ±10%. However, there are other factors that affect the NPV of these systems including capacity factor, the LMP profile used, and the operation costs. In scenarios where a NGCC power plant has a very low-capacity factor due to low electricity prices, the operational costs will be reduced and the capital costs will play a larger factor in the sensitivity of the NPV. Conversely, in areas with very large natural gas fuel prices, the operational costs will have a higher impact on the overall NPV of the system, reducing the impact of the capital costs. The impact of LMP profile is discussed in the following section.

3.4. Impact of Electricity LMP Profile on Thermal Storage Performance

The results presented so far were analyzed using historical LMP pricing data. However, NGCC+CCS systems are not expected to be widely implemented before 2040 [7,70]. Therefore, it is important to understand which LMP profiles will allow the given technology to succeed and which LMP profiles indicate that the technology is not viable. To determine the types of LMP profiles that make the technology profitable, artificial profiles were generated and characterized by two parameters: average electricity price and variability/deviation from the average price. Figure 7 shows the discharging electricity price required for each of the thermal storage configurations to have a higher NPV than NETL's B31B given an average operation price for electricity. If a LMP profile's average electricity price and average deviation fall above a configuration's breakeven line in Figure 7, the configuration would be more profitable than the base power plant for that price profile. The node data from NYISO and CAISO are also shown on the figure for comparison.

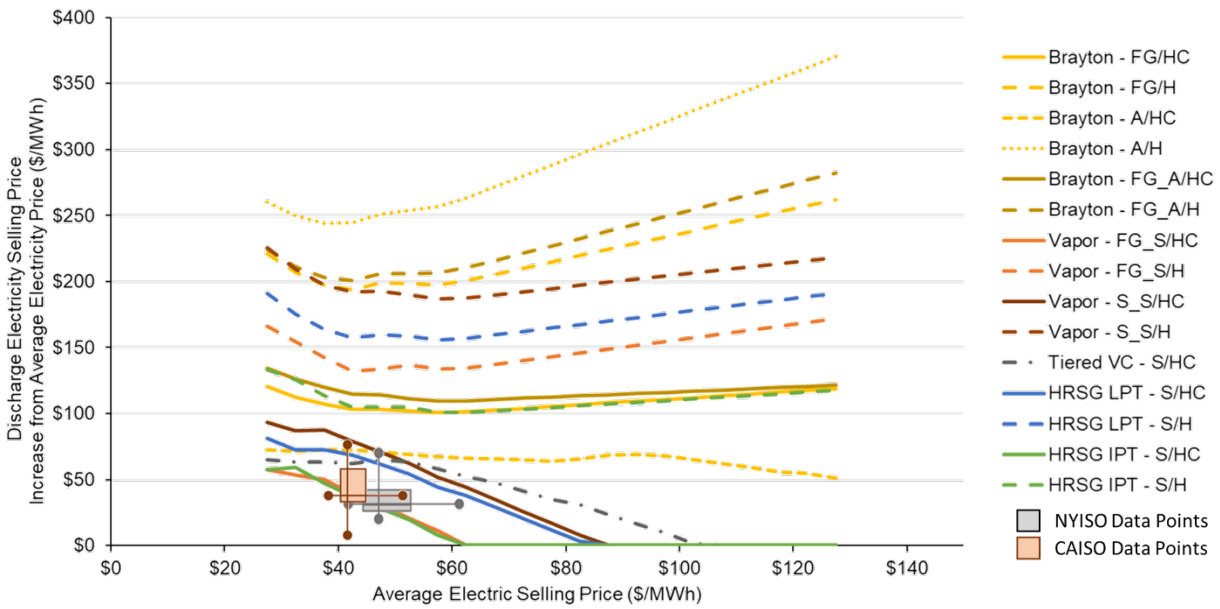

Figure 7. Discharge electricity selling price required for each thermal storage configuration to have a higher NPV than NTEL's Case B31B given an average electricity selling price. NYISO and CAISO LMP data points are also shown on the figures using 25th and 75th percentile box and whisker plots in both average electricity price and discharge electricity price directions.

This figure can be used to evaluate the economic feasibility of the thermal storage configurations compared to NETL's B31B for any new or predicted LMP profiles. For example, LMP profile data points for the NYISO and CAISO electricity markets are plotted in Figure 7 and correlate to the results found in Figure 5. As expected, the breakeven lines for the top two configurations identified in section 3.2 (Vapor – FG_S/HC and HRSG IPT – S/HC) fall above the median points for both NYISO and CAISO regions. This figure also shows that the thermal storage configurations which can operate in the boosting phase (Brayton – A/HC, Vapor - FG_S/HC, Vapor – S/HC, Tiered VC – S/HC, HRSG LPT – S/HC, and HRSG IPT – S/HC) always have a larger net power output than the base plant. As such, their breakeven lines asymptotically approach zero when the additional profits from the boosted phase are large enough to compensate for the TES capital costs. This shows that these configurations would be more economically appealing with higher mean electricity prices and/or higher price volatility, which are both considered probable in the future [71–73]. The rest of the thermal storage configurations have a positive slope because the penalty associated with charging the TES is greater than the increased power output during discharge. Therefore, as the average electricity price increases, so does the discharging electricity price needed to compensate for the difference in capital costs for these systems. The noticeable drop in discharge price between the average selling prices of $25-$40/MWh can be explained by the capacity factor of each of the systems. As mentioned previously, the operation model is designed to operate only when the plant is profitable. Each of the configurations have their own breakeven cost depending on the operation costs, but all are between $25-$40/MWh. Therefore, when the average selling price is near the breakeven price, the power plant operates less frequently, and requires higher discharge prices to be profitable.

3.5. Limitations and Future Work

The primary purpose of this study was to identify if any TES configurations could be used in combination with NGCC power plants using CCS to overcome the impact of the large heat load required by CCS solvent regeneration. While the presented research shows definite promise to multiple TES configurations, there are also some limitations that were associated with this analysis that could alter the feasibility of these TES configurations. First, the TES configurations were not fully optimized prior to the downselection process. Each configuration was evaluated with the same operation strategy and storage duration. However, optimizing the TES configurations will only increase their performance compared to the base plant. Based on the results presented, the best performing TES configurations (Vapor - FG_S/HC, HRSG IPT – S/HC, and Tiered VC – S/HC) should be optimized on a component-by-component basis (thermal storage size, charge/discharge time, turbine sizes, etc.) to ensure the maximum NPV can be generated by the system. Second, this research did not account for NGCC and CCS ramp rates. While this exclusion should not impact which TES configurations performed best since they all used the same base power plant, this assumption may affect the true NPV that was calculated. Additionally, incorporating ramp rates would allow the technologies to operate more flexibly than the four specified operation modes in this study. Further work is being done to understand the impact of realistic ramp rates on the NPV of NGCC+CCS+TES systems. Third, this research evaluated each LMP profile with perfect knowledge of the electricity prices for 24-hour time periods. Internal testing has shown this assumption will not change the ranking of TES configurations, but could impact the TES operation and associated NPV. Future work will implement a control optimization algorithm to eliminate perfect foresight and evaluate the impact of this assumption. Fourth, all configurations were evaluated using NETL's design point of 15°C for inlet air temperature for the NGCC. As ambient temperature changes, the performance of each of these configurations will also change (particularly the benefit of cold TES in cold climates). Further work is being done to understand the impact of various climates on TES operation and performance. Lastly, these technologies were evaluated using historical LMP profile data, but aren't expected to be used until 2040 [7,70]. As such, these technologies should be evaluated using future electricity LMP profiles to understand long term feasibility of these solutions. Increased renewable energy is expected to cause long periods of low electricity prices where the TES configurations that can charge independently of the NGCC will likely perform better.

4. Conclusion

Currently, fossil fuel-based power plants generate the majority of the United States' electricity and provide a reliable generation source for both base and peak power demands. However, future emissions standards are expected to require these power plants to use CCS, which has a detrimental impact on the power plant's performance. Therefore, this study evaluated fifteen TES configurations designed to overcome the operational limitation placed on the NGCC by CCS due to the large heat load required for solvent regeneration.

Results from this analysis showed that thermal storage can greatly impact the performance of a NGCC+CCS system and increase the plants profits compared to NETL's B31B. The two thermal storage configurations that performed the best were 1) a vapor compression heat pump using flue

gas heated steam as the working fluid and both hot and cold thermal storage (Vapor - FG_S/HC) and 2) removing steam before the intermediate pressure turbine and storing the hot energy in the hot storage and using cold thermal storage (HRSG IPT – S/HC). These two configurations performed better than NETL's Case B31B (NGCC+CCS) on 38.7% and 36.9% of the NYISO nodes, respectively. Additionally, a tiered vapor compression system using steam as the working fluid (Tiered VC – S/HC) performed well (third best overall) on LMP profiles with low electricity prices and low NGCC capacity factor because it can charge the hot TES independently of the NGCC. This allows the TES to charge during periods of very low electricity prices which are expected to increase in the future.

While this research shows the promising impact of using TES in combination with NGCC+CCS systems, there are some limitations that future work needs to address. These limitations include incorporating realistic ramp rates into the NGCC and CCS' operation, optimizing the unique components of each of the TES configurations (thermal storage size, charge/discharge time, turbine sizes, etc.) to increase maximum profits compared to B31B, evaluate the impact on different geographic locations on TES performance, and evaluate future LMP profile data to understand long term feasibility on these systems.

It is recommended that future research build upon the results found through this work to 1. Evaluate additional TES configurations that can charge independently of the NGCC's operation since the Tiered VC configuration performed well 2. Optimize TES configuration sizing and storage duration to achieve highest NPV possible and 3. Use simulated future electricity price signals to determine the benefit of TES for NGCC+CCS systems in future grid scenarios with increased renewable energy deployment.

CRediT authorship contribution statement

Braden J. Limb: Methodology, Software, Formal analysis, Data Curation, Writing - original draft, Visualization. **Ethan Markey:** Methodology, Software, Validation, Formal analysis, Data Curation, Writing - original draft. **Roberto Vercellino:** Methodology, Software, Validation, Formal analysis, Data Curation, Writing - original draft. **Shane Garland:** Conceptualization, Software, Validation, Funding acquisition. **Maxwell Pisciotta:** Methodology, Writing - review and editing, Resources. **Peter Psarras:** Supervision, Resources. **Daniel R. Herber:** Methodology, Software, Validation, Supervision, Funding acquisition. **Todd Bandhauer:** Conceptualization, Methodology, Validation, Supervision, Funding acquisition. **Jason C. Quinn:** Methodology, Validation, Writing - review and editing, Visualization, Supervision, Funding acquisition.

Declaration of Competing Interest

The authors declare that they have no known competing financial interests or personal relationships that could have appeared to influence the work reported in this paper.

Acknowledgements

The authors are grateful for financial support from the Department of Energy (DOE) Advanced Research Projects Agency-Energy (ARPA-E) award # DE-AR0001306. Additionally, the authors acknowledge support from Kelli Morrill, Owen Limb, Rori Limb, and Danna Quinn.

References

[1] United Nations. Adoption of the Paris Agreement, 2015.

[2] Schleussner C-F, Rogelj J, Schaeffer M, Lissner T, Licker R, Fischer EM, et al. Science and policy characteristics of the Paris Agreement temperature goal. Nat Clim Change 2016;6:827–35. https://doi.org/10.1038/nclimate3096.

[3] UNFCCC Climate Goal by Country 2017. https://www4.unfccc.int/sites/submissions/indc/Submission%20Pages/submissions.aspx (accessed April 13, 2021).

[4] Australia Climate Change Authority. Comparing countries' emissions targets n.d. https://www.climatechangeauthority.gov.au/comparing-countries-emissions-targets (accessed May 4, 2021).

[5] U.S. Environmental Protection Agency. Global Greenhouse Gas Emissions Data 2016. https://www.epa.gov/ghgemissions/global-greenhouse-gas-emissions-data (accessed April 21, 2021).

[6] Capturing carbon: Can it save us? Chem Eng News n.d. https://cen.acs.org/environment/greenhouse-gases/Capturing-carbon-save-us/97/i8 (accessed April 20, 2021).

[7] Babaee S, Loughlin DH. Exploring the role of natural gas power plants with carbon capture and storage as a bridge to a low-carbon future. Clean Technol Environ Policy 2018;20:379–91. https://doi.org/10.1007/s10098-017-1479-x.

[8] Mignone BK, Showalter S, Wood F, McJeon H, Steinberg D. Sensitivity of natural gas deployment in the US power sector to future carbon policy expectations. Energy Policy 2017;110:518–24. https://doi.org/10.1016/j.enpol.2017.08.012.

[9] Du Y, Gao T, Rochelle GT, Bhown AS. Zero- and negative-emissions fossil-fired power plants using CO2 capture by conventional aqueous amines. Int J Greenh Gas Control 2021;111:103473. https://doi.org/10.1016/j.ijggc.2021.103473.
[10] Chao C, Deng Y, Dewil R, Baeyens J, Fan X. Post-combustion carbon capture. Renew Sustain Energy Rev 2021;138:110490. https://doi.org/10.1016/j.rser.2020.110490.
[11] International Energy Agency. CCUS in Power – Analysis. IEA n.d. https://www.iea.org/reports/ccus-in-power (accessed June 6, 2021).
[12] NS Energy. What are the top carbon capture and storage projects around the world? n.d. https://www.nsenergybusiness.com/features/top-carbon-capture-storage-projects/ (accessed June 2, 2021).
[13] U.S. Energy Information Administration (EIA). More than 100 coal-fired plants have been replaced or converted to natural gas since 2011 - Today in Energy n.d. https://www.eia.gov/todayinenergy/detail.php?id=44636 (accessed June 1, 2021).
[14] U.S. Energy Information Administration (EIA). More U.S. coal-fired power plants are decommissioning as retirements continue - Today in Energy n.d. https://www.eia.gov/todayinenergy/detail.php?id=40212 (accessed June 1, 2021).
[15] Jacobson, Mark Z. The 7 reasons why nuclear energy is not the answer to solve climate change | Heinrich Böll Stiftung | Brussels office - European Union. Heinrich-Böll-Stift n.d. https://eu.boell.org/en/2021/04/26/7-reasons-why-nuclear-energy-not-answer-solve-climate-change (accessed May 15, 2021).
[16] Wilkerson, Jordan. Reconsidering the Risks of Nuclear Power. Sci News 2016. https://sitn.hms.harvard.edu/flash/2016/reconsidering-risks-nuclear-power/ (accessed May 15, 2021).
[17] Stauffer, Nancy W. Building nuclear power plants. Mass Inst Technol n.d. https://energy.mit.edu/news/building-nuclear-power-plants/ (accessed May 15, 2021).
[18] Gürsan C, de Gooyert V. The systemic impact of a transition fuel: Does natural gas help or hinder the energy transition? Renew Sustain Energy Rev 2021;138:110552. https://doi.org/10.1016/j.rser.2020.110552.
[19] Delborne JA, Hasala D, Wigner A, Kinchy A. Dueling metaphors, fueling futures: “Bridge fuel” visions of coal and natural gas in the United States. Energy Res Soc Sci 2020;61:101350. https://doi.org/10.1016/j.erss.2019.101350.
[20] Global CCS Institute. CO2 Capture Technologies - Post Combustion Capture (PCC). 2012.
[21] National Renewable Energy Laboratory. Renewable Electricity Futures Study. Volume 1: Exploration of High-Penetration Renewable Electricity Futures 2012:280.
[22] Leslie M. The Next Energy Battle: Cheap Natural Gas versus Renewables. Engineering 2021;7:133–5. https://doi.org/10.1016/j.eng.2020.12.008.
[23] Tait P, Buschle B, Ausner I, Valluri P, Wehrli M, Lucquiaud M. A pilot-scale study of dynamic response scenarios for the flexible operation of post-combustion CO2 capture. Int J Greenh Gas Control 2016;48:216–33. https://doi.org/10.1016/j.ijggc.2015.12.009.
[24] Chen Q, Kang C, Xia Q, Kirschen D s. Optimal Flexible Operation of a CO2 Capture Power Plant in a Combined Energy and Carbon Emission Market. IEEE Trans Power Syst 2012;27:1602–9.
[25] Oates DL, Versteeg P, Hittinger E, Jaramillo P. Profitability of CCS with flue gas bypass and solvent storage. Int J Greenh Gas Control 2014;27:279–88. https://doi.org/10.1016/j.ijggc.2014.06.003.

[26] Cohen SM, Rochelle GT, Webber ME. Optimal operation of flexible post-combustion CO2 capture in response to volatile electricity prices. Energy Procedia 2011;4:2604–11. https://doi.org/10.1016/j.egypro.2011.02.159.
[27] Cohen S, Rochelle G, Webber M. Optimizing post-combustion CO2 capture in response to volatile electricity prices. Int J Greenh Gas Control 2012;8:180–95. https://doi.org/10.1016/j.ijggc.2012.02.011.
[28] Cohen S, Rochelle G, Webber M. Optimal CO2 Capture Operation in an Advanced Electric Grid. Energy Procedia 2013;37:2585–94. https://doi.org/10.1016/j.egypro.2013.06.142.
[29] OECD. Effective Carbon Rates 2021: Pricing Carbon Emissions through Taxes and Emissions Trading. OECD; 2021. https://doi.org/10.1787/0e8e24f5-en.
[30] BloombergNEF. Carbon Offset Prices Could Increase Fifty-Fold by 2050. BloombergNEF 2022. https://about.bnef.com/blog/carbon-offset-prices-could-increase-fifty-fold-by-2050/ (accessed January 31, 2022).
[31] Bhat P. Carbon needs to cost at least $100/tonne now to reach net zero by 2050: Reuters poll. Reuters 2021.
[32] Ajiwibowo M, Darmawan A, Aziz M. A conceptual chemical looping combustion power system design in a power-to-gas energy storage scenario. Int J Hydrog Energy 2018;44. https://doi.org/10.1016/j.ijhydene.2018.11.177.
[33] Szima S, Cormos A-M, Cormos C-C. Flexible Hydrogen and Power Co - generation based on Dry Methane Reforming with Carbon Capture. In: Friedl A, Klemeš JJ, Radl S, Varbanov PS, Wallek T, editors. Comput. Aided Chem. Eng., vol. 43, Elsevier; 2018, p. 1281–6. https://doi.org/10.1016/B978-0-444-64235-6.50225-4.
[34] Davison J, Arienti S, Cotone P, Mancuso L. Co-production of hydrogen and electricity with CO2 capture. Energy Procedia 2009;1:4063–70. https://doi.org/10.1016/j.egypro.2009.02.213.
[35] Hu Y, Li X, Li H, Yan J. Peak and off-peak operations of the air separation unit in oxy-coal combustion power generation systems. Appl Energy 2013;112:747–54. https://doi.org/10.1016/j.apenergy.2012.12.001.
[36] Mitchell C, Avagyan V, Chalmers H, Lucquiaud M. An initial assessment of the value of Allam Cycle power plants with liquid oxygen storage in future GB electricity system. Int J Greenh Gas Control 2019;87:1–18. https://doi.org/10.1016/j.ijggc.2019.04.020.
[37] Domenichini R, Mancuso L, Ferrari N, Davison J. Operating Flexibility of Power Plants with Carbon Capture and Storage (CCS). Energy Procedia 2013;37:2727–37. https://doi.org/10.1016/j.egypro.2013.06.157.
[38] David Yellen. Carbon capture and the Allam Cycle: The future of electricity or a carbon pipe(line) dream? Atl Counc 2020. https://www.atlanticcouncil.org/blogs/energysource/carbon-capture-and-the-allam-cycle-the-future-of-electricity-or-a-carbon-pipeline-dream/ (accessed January 31, 2022).
[39] Paudel A, Bandhauer T. Techno-economic analysis of waste heat recovery systems for wet-cooled combined cycle power plants. Appl Therm Eng 2018;143:746–58. https://doi.org/10.1016/j.applthermaleng.2018.07.138.
[40] Eveloy V, Rodgers P, Popli S. Power generation and cooling capacity enhancement of natural gas processing facilities in harsh environmental conditions through waste heat utilization. Int J Energy Res 2014;38:1921–36. https://doi.org/10.1002/er.3197.

[41] Mohapatra AK, Sanjay. Thermodynamic assessment of impact of inlet air cooling techniques on gas turbine and combined cycle performance. Energy 2014;68:191–203. https://doi.org/10.1016/j.energy.2014.02.066.
[42] Li D, Hu Y, He W, Wang J. Dynamic modelling and simulation of a combined-cycle power plant integration with thermal energy storage. 2017 23rd Int. Conf. Autom. Comput. ICAC, 2017, p. 1–6. https://doi.org/10.23919/IConAC.2017.8081972.
[43] Gil A, Medrano M, Martorell I, Lázaro A, Dolado P, Zalba B, et al. State of the art on high temperature thermal energy storage for power generation. Part 1—Concepts, materials and modellization. Renew Sustain Energy Rev 2010;14:31–55. https://doi.org/10.1016/j.rser.2009.07.035.
[44] Medrano M, Gil A, Martorell I, Potau X, Cabeza LF. State of the art on high-temperature thermal energy storage for power generation. Part 2—Case studies. Renew Sustain Energy Rev 2010;14:56–72. https://doi.org/10.1016/j.rser.2009.07.036.
[45] Chang J, Lee G, Adams D, Ahn H, Lee J, Oh M. Multiscale modeling and integration of a combined cycle power plant and a two-tank thermal energy storage system with gPROMS and SimCentral. Korean J Chem Eng 2021;38:1333–47. https://doi.org/10.1007/s11814-021-0789-1.
[46] Malta Inc. Malta's Electro-Thermal Energy Storage System: A Better Way to Enable Cleaner Reliable Electricity on the Grid. Malta Inc n.d. https://www.maltainc.com/our-solution (accessed January 31, 2022).
[47] Smallbone A, Jülch V, Wardle R, Roskilly AP. Levelised Cost of Storage for Pumped Heat Energy Storage in comparison with other energy storage technologies. Energy Convers Manag 2017;152:221–8. https://doi.org/10.1016/j.enconman.2017.09.047.
[48] Gkoutzamanis V, Chatziangelidou A, Efstathiadis T, Kalfas A, Traverso A, Chiu JNW. Thermal Energy Storage For Gas Turbine Power Augmentation. J Glob Power Propuls Soc 2019;3:592–608. https://doi.org/10.33737/jgpps/110254.
[49] Barigozzi G, Perdichizzi A, Gritti C, Guaiatelli I. Techno-economic analysis of gas turbine inlet air cooling for combined cycle power plant for different climatic conditions. Appl Therm Eng 2015;82:57–67. https://doi.org/10.1016/j.applthermaleng.2015.02.049.
[50] Palestra N, Barigozzi G, Perdichizzi A. Inlet Air Cooling Applied to Combined Cycle Power Plants: Influence of Site Climate and Thermal Storage Systems. J Eng Gas Turbines Power 2008;130. https://doi.org/10.1115/1.2771570.
[51] Zhang H, Baeyens J, Cáceres G, Degrève J, Lv Y. Thermal energy storage: Recent developments and practical aspects. Prog Energy Combust Sci 2016;53:1–40. https://doi.org/10.1016/j.pecs.2015.10.003.
[52] Ela E, Billimoria F, Ragsdale K, Moorty S, O'Sullivan J, Gramlich R, et al. Future Electricity Markets: Designing for Massive Amounts of Zero-Variable-Cost Renewable Resources. IEEE Power Energy Mag 2019;17:58–66. https://doi.org/10.1109/MPE.2019.2933281.
[53] Gomez T, Herrero I, Rodilla P, Escobar R, Lanza S, de la Fuente I, et al. European Union Electricity Markets: Current Practice and Future View. IEEE Power Energy Mag 2019;17:20–31. https://doi.org/10.1109/MPE.2018.2871739.
[54] James R, Zoelle A, Keairns D, Turner M, Woods M, Kuehn N. Cost And Performance Baseline for Fossil Energy Plants Volume 1: Bituminous Coal and Natural Gas To Electricity. National Energy Technology Laboratory (NETL); 2019.

[55] Shell CANSOLV® CO_2 Capture System n.d. https://www.shell.com/business-customers/catalysts-technologies/licensed-technologies/emissions-standards/tail-gas-treatment-unit/cansolv-co2.html (accessed August 20, 2021).
[56] Wilcox J. Carbon Capture. New York: Springer-Verlag; 2012. https://doi.org/10.1007/978-1-4614-2215-0.
[57] Carnegie Mellon University (CMU). Integrated Environmental Control Model n.d. https://www.cmu.edu/epp/iecm/ (accessed March 15, 2021).
[58] Storworks Power. Economic Benefits. Storworks n.d. https://storworks.com/economic-benefits/ (accessed April 15, 2021).
[59] Solids - Specific Heats n.d. https://www.engineeringtoolbox.com/specific-heat-solids-d_154.html (accessed September 13, 2022).
[60] Solids, Liquids and Gases - Thermal Conductivities n.d. https://www.engineeringtoolbox.com/thermal-conductivity-d_429.html (accessed September 13, 2022).
[61] National Renewable Energy Laboratory. 2020 Electricity Annual Technology Baseline n.d. https://atb-archive.nrel.gov/electricity/2020/data.php (accessed October 1, 2020).
[62] U.S. Energy Information Administration (EIA). Annual Energy Outlook 2021 2021. https://www.eia.gov/outlooks/aeo/ (accessed March 6, 2021).
[63] U.S. Bureau of Labor Statistics. Consumer Price Index Data n.d. https://data.bls.gov/timeseries/CUUR0000SA0 (accessed December 15, 2020).
[64] New York Independent System Operator. Energy Market & Operational Data - NYISO n.d. https://www.nyiso.com/energy-market-operational-data (accessed October 30, 2020).
[65] California Independent System Operator. California ISO OASIS n.d. http://oasis.caiso.com/ (accessed October 30, 2020).
[66] U.S. Energy Information Administration (EIA). New York Natural Gas Prices n.d. https://www.eia.gov/dnav/ng/ng_pri_sum_dcu_sny_m.htm (accessed October 30, 2020).
[67] Nunes P, Brito MC. Displacing natural gas with electric vehicles for grid stabilization. Energy 2017;141:87–96. https://doi.org/10.1016/j.energy.2017.09.064.
[68] Papaefthymiou G, Grave K, Dragoon K. Flexibility options in electricity systems. 2014.
[69] Hunter CA, Penev MM, Reznicek EP, Eichman J, Rustagi N, Baldwin SF. Techno-economic analysis of long-duration energy storage and flexible power generation technologies to support high-variable renewable energy grids. Joule 2021;5:2077–101. https://doi.org/10.1016/j.joule.2021.06.018.
[70] EPA's Office of Research & Development. The Role of Natural Gas Power Plants with Carbon Capture and Storage in a Low-Carbon Future n.d. https://cfpub.epa.gov/si/si_public_record_report.cfm?Lab=NRMRL&dirEntryId=338530 (accessed May 15, 2021).
[71] Frew B, Stephen G, Lau J, Ela E, Singhal N, Bloom A, et al. Impacts of Price Formation Efforts Considering High Renewable Penetration Levels and System Resource Adequacy Targets. 2020. https://doi.org/10.2172/1659808.
[72] Frew B, Brinkman G, Denholm P, Narwade V, Stephen G, Bloom A, et al. Impact of operating reserve rules on electricity prices with high penetrations of renewable energy. Energy Policy 2021;156:112443. https://doi.org/10.1016/j.enpol.2021.112443.
[73] Rai A, Nunn O. On the impact of increasing penetration of variable renewables on electricity spot price extremes in Australia. Econ Anal Policy 2020;67:67–86. https://doi.org/10.1016/j.eap.2020.06.001.